Application Specific Optical Fibers

Bishnu P. Pal
Indian Institute of Technology Delhi
Physics Department
New Delhi: 110016
India

1. Introduction

Optical fiber technology was considered to be a major driver behind the information technology revolution and the huge progress on global telecommunications that has been witnessed in recent years. Fiber optic telecommunication is now taken for granted in view of its wide-ranging application as the most suitable singular transmission medium for voice, video, and data signals. Indeed, optical fibers have now penetrated virtually all segments of telecommunication networks - be it trans-oceanic, transcontinental, inter-city, metro, access, campus, or on-premise [Pal, 2006]. Initial R&D revolution in this field had centered on achieving optical *transparency* in terms of exploitation of the *low-loss* and *low-dispersion* transmission wavelength windows of high-silica optical fibers. The earliest optical fiber communication systems exploited the first low loss wavelength window centered on 820 nm of silica with graded index multimode fibers as the transmission media. However, primarily due to unpredictable nature of the bandwidth of jointed multimode fiber links, since early-1980s the system focus had shifted to single-mode fibers. This was accentuated by the discovery of the zero material dispersion characteristic of silica fibers, which occurs at a wavelength of 1280 nm [Payne & Gambling, 1975] in close proximity to its second low loss wavelength window centered at 1310 nm. The next revolution in lightwave communication took place when *broadband* optical fiber *amplifiers* in the form of erbium doped fiber amplifiers (EDFA) were developed in 1987 [Mears et al, 1987], whose operating wavelengths fortuitously coincided with the lowest loss transmission window of silica fibers centered at 1550 nm [Miye et al, 1979] and heralded the emergence of the era of *dense wavelength division multiplexing* (DWDM) technology in the mid-1990s [Kartapoulos, 2000]. Recent development of the so-called low water peak fibers like AllWave™ and SMF-28e™ fibers, which are devoid of the characteristic OH$^-$ loss peak (centered at 1380 nm) extended the low loss wavelength window in high-silica fibers from 1280 nm (235 THz) to 1650 nm (182 THz) thereby offering, in principle, an enormously broad 53 THz of optical transmission bandwidth to be potentially tapped through DWDM technique! State-of-the-art technology has already demonstrated exploitation and utilization of 25 ~ 30 THz optical bandwidth. The emergence of DWDM technology has also driven the development of various specialty fibers and all-fiber components for seamless growth of the lightwave communication technology. These application-specific fibers were required to address new issues/features such as broadband dispersion compensation, realization of specialized components such as

fiber couplers for multiplexing pump and signal wavelengths required in configuring fiber amplifiers, erbium doped fibers for realizing EDFAs, realization of wavelength sensitive in-fiber grating-based components, low sensitivity to nonlinear impairments with propagation, and so on. There has also been a resurgence of interest amongst researchers to design and fabricate an exotic class of special fibers - fibers in which transmission losses of the material would not be a limiting factor while nonlinearity and dispersion characteristics could be conveniently tailored to achieve certain application-specific fibers, not necessarily for telecommunication applications only. Research targeted towards such fiber designs led to the emergence of a new class of fibers, broadly referred to as *microstructured optical fibers* (MOF), which are characterized by wavelength-scale periodic refractive index features across its physical cross-section resulting in *photonic bandgaps* when appropriately designed. These features could be periodically located air holes/low refractive index regions in the cladding region, which surround the central core region, which could be of higher or lower refractive index than the average refractive index of the cladding region. Due to the large degree of design freedom and flexibility and also strong dependence on wavelength of the mode effective index, microstructured fibers have opened up a variety of new applications such as spectral broadening of a short pulse due to extreme nonlinear effects after propagating through a MOF resulting in generation of supercontinuum light, wide band transmission, high power delivery, endlessly single mode, very large or very small mode effective area, low-loss guidance of light in an air core and so on. In this chapter we would attempt to describe several application-specific specialty fibers and include some results of our own work in this direction.

2. Optical transparency

2.1 Loss spectrum

Loss spectrum, *dispersion* and *nonlinear propagation effects* are the three most important propagation characteristics of any signal transmitting single-mode optical fiber in the context of modern optical telecommunication. An illustrative example of the loss spectrum of a state-of-the-art commercially available conventional ITU[1] recommended standard G.652 type of single-mode fiber is shown in Fig. 1 [Pal, 2006]. Except for portion of the loss spectrum around 1380 nm at which a peak appears due to absorption by minute traces of OH^- present in the fiber, the rest of the spectrum in a G.652 fiber could be well described through a wavelength dependence as $A\lambda^{-4}$ meaning thereby that signal loss in such fibers is essentially dominated by Rayleigh scattering; A is the Rayleigh scattering coefficient. With GeO_2 as the dopant and relative core-cladding index difference $\Delta \sim 0.37\%$, where $\Delta \sim [(n_c - n_{cl})/n_{c,cl}]$ estimated Rayleigh scattering loss in a high-silica fiber is about 0.18 – 0.2 dB/km at 1550 nm; $n_{c,cl}$ correspond to core and cladding refractive indices, respectively. Superimposed on this curve over the wavelength range 1360 ~ 1460 nm (often referred to as the E-band) is a dotted curve without the peak but overlapping otherwise with rest of the loss spectrum; this modified spectrum represents a sample corresponding to a low water peak fiber like AllWave™ or SMF-28e™ fiber. In real-world systems, however, there are other sources of loss, which are required to be accounted for, on case-to-case basis,

[1]ITU stands for International Telecommunication Union
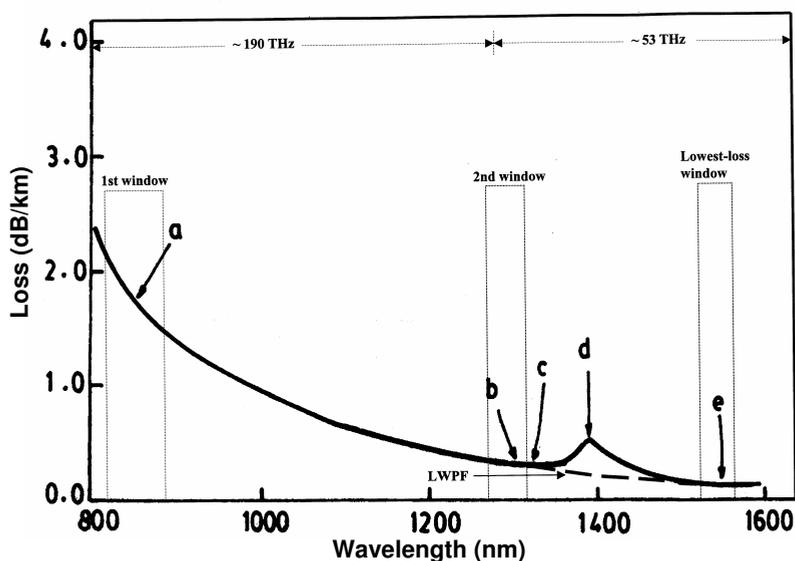
Fig. 1. Loss spectrum (full curve) of a state-of-the-art G.652 type single-mode fiber, e.g. SMF-28 (adapted from Corning product catalogue©Corning Inc.): (a) 1.81 dB/km at 850 nm, (b) 0.35 dB/km at 1300 nm, (c) 0.34 dB/km at 1310 nm, (d) 0.55 dB/km at 1380 nm, (e) 0.19 dB/km at 1550 nm. The dashed portion of the curve corresponds to that of a low water peak fiber due to reduction of the OH⁻ peak in enhanced SMF; theoretical transmission bandwidths at different low loss spectral windows are also shown [After Pal, 2006; ©2006 Elsevier Press].

and which could add up to more than the inherent loss of the fiber. Examples of these potential sources are cabling-induced losses due to microbending, bend-induced losses along a fiber route due to wrong installation procedures, losses due to splices and connectors including those involving insertion of various components in a fiber link. Several of these also depend to a certain extent on the refractive index profile of the fiber in question. Detailed studies have indicated that these extraneous sources of loss could be addressed by optimizing mode field radius (W_P, known as Petermann spot size/mode field radius) and effective cut-off wavelength (λ_{ce}) [Pal, 1995]. The parameter W_P effectively determines transverse offset-induced loss at a fiber splice as well as loss-sensitivity to microbends and λ_{ce} essentially determines sensitivity to bend-induced loss in transmission. For operating at 1310 nm, optimum values of these parameters were found to range between 4.5 and 5.5 µm and between 1100 and 1280 nm, respectively. An indirect way to test that λ_{ce} indeed falls within this range is ensured if the measured excess loss of 100 turns of the fiber loosely wound around a cylindrical mandrel of diameter 7.5 cm falls below 0.1 dB at 1310 nm and below 1.0 dB at 1550 nm [Pal, 1995].

2.2 Dispersion spectrum

Chromatic dispersion, whose very name implies that it is dependent on wavelength and whose magnitude is a measure of the information transmission capacity of a single-mode fiber, is another important transmission characteristic (along with loss) and it arises because

of the dispersive nature of an optical fiber due to which the group velocity of a propagating signal pulse becomes a function of frequency (usually referred to as *group velocity dispersion* [GVD] in the literature), which limits the number of pulses that can be sent through the fiber per unit time. This phenomenon of GVD induces frequency chirp to a propagating pulse, meaning thereby that *leading edge* of the propagating pulse differs in frequency from the *trailing edge* of the pulse. The resultant frequency chirp [i.e. $\omega(t)$] leads to inter-symbol interference (ISI), in the presence of which the receiver fails to resolve the digital signals as individual pulses when the pulses are transmitted too close to each other [Ghatak & Thyagarajan, 1998]. Thus the signal pulses though started, as individually distinguishable pulses at the transmitter, may become indistinguishable at the receiver depending on the amount of chromatic dispersion-induced broadening introduced by the fiber after propagating through a given length of the fiber (see Fig. 2). For quantitative purposes, dispersion is expressed through dispersion coefficient (*D*) defined as [Thyagarajan & Pal, 2007]

$$D = \frac{1}{L}\frac{d\tau}{d\lambda_0} = -\frac{\lambda_0}{c}\frac{d^2 n_{eff}}{d\lambda_0^2} \tag{1}$$

where τ is the group delay and n_{eff} is the mode effective index of the fundamental mode in a single-mode fiber. It can be shown that the total dispersion coefficient (D_T) is given to a very good accuracy by the algebraic sum of two components $D_T \cong D_M + D_{WG}$ where D_M and D_{WG} correspond to material and waveguide components of *D*, respectively. A plot of typical dispersion spectrum is shown in Fig. 3. It can be seen from it that D_{WG} is all along negative and while sign of D_M changes from negative to positive (going through zero at a wavelength of ~ 1280 nm [Payne & Gambling, 1975]) with increase in wavelength. The two components of *D* cancel each other at a wavelength near about 1300 nm, which is referred to as the *zero dispersion wavelength* (λ_{ZD}) and it is a very important design parameter of single- mode fibers. Realization of this fact led system operators to choose the operating wavelength
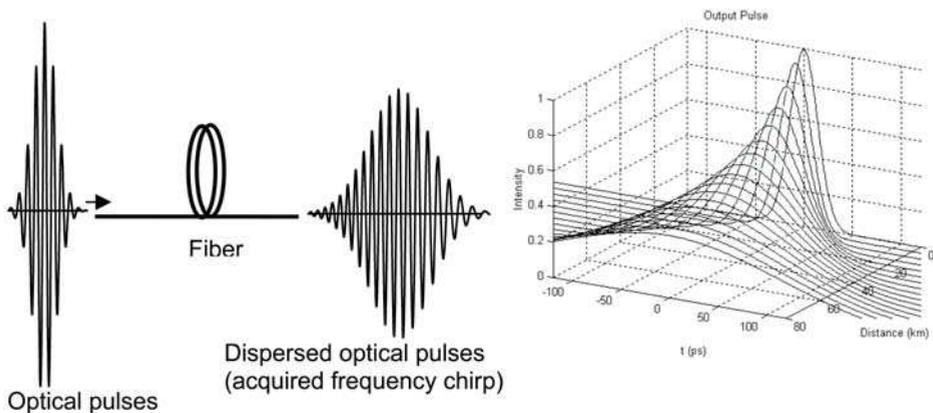

Fig. 2. a) Schematic showing dispersion of a Gaussian input pulse with propagation through a dispersive medium e.g. an optical fiber; frequency chirp is apparent in the dispersed pulse; b) Calculated dispersion induced broadening of a Gaussian pulse [Results courtesy Sonali Dasgupta]
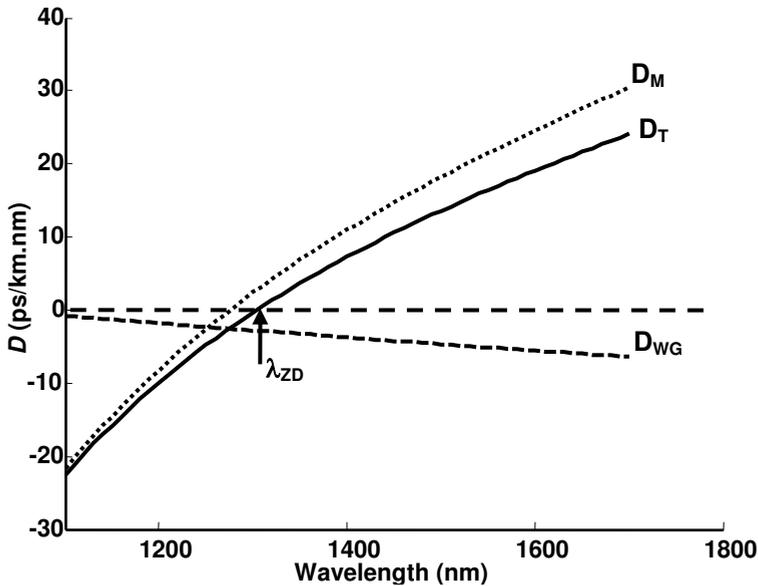
Fig. 3. Dispersion coefficient, D as a function of wavelength of a typical G.652 type fiber; D_M and D_{WG} correspond to material and waveguide components, respectively of total D while λ_{ZD} refers to wavelength for zero total dispersion [After Thyagarajan and Pal, 2006; ©2006 Springer Verlag].

of first generation single-mode fibers as 1310 nm. These fibers optimized for transmission at 1310 nm are now referred to as G.652 fibers as per ITU standards; millions of kilometers of these fibers are laid underground all over the world. Though it appears that if operated at λ_{ZD} one might get infinite transmission bandwidth, in reality zero dispersion is only an approximation (albeit a very good approximation) because it simply signifies that only the second order dispersive effects would be absent. In fact as per ITU recommendations, SMF-28 type of standard G.652 fibers qualify for deployment as telecommunication media provided at the 1310 nm wavelength, its D_T is < 3.5 ps/(nm.km). At a wavelength around λ_{ZD} third order dispersion would determine the net dispersion of a pulse. In the absence of second order dispersion, pulse dispersion is quantitatively determined by the dispersion slope S_0 at $\lambda = \lambda_{ZD}$. A knowledge of D and S_0 enables determination of dispersion (D) at any arbitrary wavelength within a transmission window e.g. EDFA band in which D in G.652 fibers varies approximately linearly with the operating wavelength λ_0 [Pal, 2006]. Besides pulse broadening, since the energy in the pulse gets reduced within its time slot, the corresponding signal to noise ratio (SNR) will decrease, which could be compensated by increasing the power in the input pulses. This additional power requirement is termed as *dispersion power penalty* [Thyagarajan & Pal, 2007]. For 1 dB dispersion power penalty at the wavelength of 1550 nm, we can write the following inequality as a design relation for estimating maximum allowed dispersion

$$B^2.D.L \leq 10^5 \text{ Gb}^2.\text{ps/nm} \tag{2}$$

where B is measured in Gbits, D in ps/(nm.km) and L in km [Pal, 2006; Thyagarajan & Pal, 2007]. Based on Eq. (2), Table I lists the maximum allowed dispersion for different standard bit rates for tolerating a dispersion power penalty of 1 dB.

Data rate (B)	Maximum allowed dispersion ($D.L$)
2.5 Gb/s (OC-48)* 10 Gb/s (OC-192) 40 Gb/s (OC-768)	~ 16000 ps/nm ~ 1000 ps/nm ~ 60 ps/nm

*OC stands for Optical Channels, which are standards for DWDM systems

Table I. Maximum allowed dispersion at different standard signal transmission rates

2.3 Nonlinear propagation effects

With the emergence of DWDM transmission, a transmission fiber is typically required to handle large power density and long interaction lengths due to transmission of multiple channels over long fiber lengths. In view of this, nonlinear propagation effects have become yet another important transmission characteristic of an optical fiber. It is well known that under the influence of intense electromagnetic fields (comparable to the inter-atomic fields that exist in the propagating medium) a fiber may exhibit certain nonlinear effects [Agrawal, 2007]. This nonlinear response of the fiber could be mathematically described through the following nonlinear relation between P and E, where P represents polarization induced by the electric field E of the propagating em field:

$$P = \varepsilon_0 \left(\chi^{(1)} E + \chi^{(2)} EE + \chi^{(3)} EEE + ... \right) \qquad (3)$$

where ε_0 is vacuum permittivity and $\chi^{(n)}$ is the nonlinear susceptibility of the medium. In silica, $\chi^{(2)}$ is absent while $\chi^{(3)}$ is finite, which is the major contributor to nonlinear effects in silica-based optical fibers. A consequence of this finite $\chi^{(3)}$ is that it leads to an intensity dependent refractive index of silica as

$$n^{NL} = n_1 + n_2 I \qquad (4)$$

where n_1 is the linear part of the fiber core refractive index and n_2 (~ 3.2 x 10^{-20} m²/W in silica as measured at 515 nm through self-phase modulation (SPM) technique; at the 1550 nm wavelength region it is usually less by ~10% [Agrawal, 2007])) is the nonlinear component of the nonlinear refractive index, related to $\chi^{(3)}$ through [Ghatak & Thyagarajan, 1998]

$$n_2 = \frac{3}{4} \frac{\chi^{(3)}}{c \varepsilon_0 n_1^2} \qquad (5)$$

and I is the intensity of the propagating em wave. For describing nonlinear effects in a fiber, often a parameter known as γ, which is defined through

$$\gamma = \frac{2\pi}{\lambda} \frac{n_2}{A_{eff}} \qquad (6)$$

is used, where [Agrawal, 2007]

$$A_{eff} = \frac{\left[\int\limits_0^\infty\int\limits_0^{2\pi} E^2(r)\,r\,dr\,d\varphi\right]^2}{\int\limits_0^\infty\int\limits_0^{2\pi} E^4(r)\,r\,dr\,d\varphi} \qquad (7)$$

is known as the mode effective area of a fiber. The parameter $\gamma \sim 1/(W.km)$ in a standard fiber like SMF-28 (of Corning Inc.). Its value could be enhanced either through smaller A_{eff} (obtainable through appropriate fiber designs) or choice of the glass materials or both. Values as large as 20 times that of SMF-28 has been reported in certain fibers through these routes [Okuno et al, 1999; Monro, 2006]. Often the fundamental LP_{01} mode of a single-mode fiber is approximately describable by a Gaussian distribution with a spot size (or mode field radius) of ω_0; in that case $\pi\omega_0^2$ would yield A_{eff} [Ghatak & Thyagarajan, 1998; Agrawal, 2007]. For simple estimations, we may consider ω_0 to be ~ 5 µm for a typical single-mode fiber at the operating wavelength of 1550 nm and hence $A_{eff} \sim 75 - 80$ µm^2 $\Rightarrow$ for a propagating power of ~ 100 µW across this cross-section of the fiber, net intensity would be ~ 106 W/m^2, resulting in a net change (= $n_2 I$) in refractive index of the fiber $\sim 3.2 \times 10^{-14}$, which though small in magnitude could lead to substantial nonlinear effect in a fiber. This is because the typical fiber lengths encountered by a propagating optical signal could be few tens to hundreds of kilometers. Nonlinear effects in a fiber could be broadly classified into two domains depending on the physical mechanism involved: refractive index related effects like self-phase modulation (SPM), cross-phase modulation (XPM), and four wave mixing (FWM) or stimulated scattering effects like stimulated Brillouin scattering (SBS), stimulated Raman scattering (SRS), and soliton self frequency shift [Agrawal, 2007]. For example, FWM could lead to generation of new waves of different wavelengths in a DWDM link. If there are N propagating signal channels, number of new waves generated [Li, 1995] due to FWM would be $\sim N^2(N - 1)/2$. In view of this, cross coupling of power between these waves/side-bands could lead to depletion of power from the signal channels and hence could result in lowering of signal to noise ratio in a particular signal channel. Detailed analyses show that FWM effect could be substantially reduced if the fiber is so designed that signals experience a finite dispersion within the fiber and/ or channel spacing is large in a DWDM stream. As an example, for a single-mode fiber having average loss of 0.25 dB/km at 1.55 µm, FWM induced power penalty in terms of the ratio of generated power [at the new frequency ω_1 (= $\omega_3 + \omega_4 - \omega_2$)] to the output power after a length of 100 km of the fiber for a channel spacing of 1 nm is $\sim - 25$ dB for $D = 0$ ps/(nm.km), $\sim - 47$ dB for $D = 1$ ps/(nm.km), and $\sim - 70$ dB for $D = 17$ ps/(nm.km); if the channel spacing is reduced to 0.5 nm, the corresponding power penalties are $\sim - 25$ dB, $\sim - 35$ dB, and $\sim - 58$ dB, respectively [Li, 1995]. Thus non-linear optical effects are important issues required to be accounted for in a DWDM communication systems of today. As per ITU standards, in a DWDM stream, signal channels are required to be equally spaced. One of the important parameters often considered in designing DWDM systems is known as spectral efficiency (*SE*), which is defined as the ratio of bit rate to channel spacing. Since, bit rate cannot be increased arbitrarily due to constraints imposed by electron mobility, *SE* could be enhanced through smaller and smaller channel spacing and hence in that context nonlinear effects like FWM becomes an important issue. For DWDM applications, fiber designers came up with new designs for the signal fiber for low-loss and dedicated DWDM signal transmission at the 1550 nm band, which were generically named as non-zero dispersion shifted fibers (NZ-

DSF). For a while, in between there was a move to deploy single-mode fibers with $D \sim 0$ at the 1550 nm band to take simultaneous advantage of lowest transmission loss in silica fibers in that band. Such fibers were known as dispersion shifted fibers (DSF). However, they were found to be of no use for DWDM transmission because nonlinear effects would be significantly high due to D being 0 in these fibers! These fibers were designed to substantially suppress nonlinear effects like FWM by allowing each of the DWDM signals to experience a finite amount of dispersion during propagation [Pal, 2006]. ITU has christened such fibers as G.655 fibers, which should exhibit dispersion $2 \le D$ (ps/(nm.km)) ≤ 6 in the 1550 nm band in order to detune the phase matching condition required for detrimental nonlinear propagation effects like four-wave mixing (FWM) and cross-phase modulation (XPM) to take place during multi-channel transmission of DWDM signals.

3. Emergence of amplifiers

3.1 Fiber amplifiers

In the late 1980s typical state-of-the-art repeater-less transmission distances were about 40-50 kms @ 560 Mb/s transmission rate. Maximum launched optical power into a fiber was below 100 μW, it was difficult to improve system lengths any further and use of electronic repeaters became inevitable. At a repeater, the so-called 3**R**-regeneration functions (*re-amplification, retiming, and reshaping*) are performed in the electric domain on the incoming attenuated as well as distorted (due to dispersion) signals after detection by a photo-detector and before the revamped signals are fed to a laser diode drive circuits, wherefrom these cleaned optical pulses are re-injected in to next section of the fiber link. However, these complex functions required unit replacement in case of network capacity upgrades because electronic components are bit rate sensitive. By mid-1980s, it was felt that *an optical amplifier is needed to bypass this electronic bottleneck.* Fortuitously in 1986, the Southampton University research group in England reported success in incorporating rare earth trivalent erbium ions into host silica glass during fiber fabrication [Mears et al, 1986]; Erbium is known to have strong fluorescence at 1550 nm. Subsequently, the same group demonstrated that excellent noise and gain performance is feasible in a large part of the 1550 nm window with erbium-doped silica fibers [Mears et al, 1987], which ushered in the era of erbium doped fiber amplifiers (EDFA) and DWDM networks; EDFAs went commercial by 1996. Absorption bands most suitable as pump for obtaining amplification of signals at the 1550 nm wavelength region are 980 nm and 1480 nm wavelengths although 980 is a more popular choice; in Fig. 4 a schematic of an EDFA is shown. When pumped at either of these wavelengths, an erbium doped fiber was found to amplify signals over a band of almost 30 $\sim$ 35 nm extending from 1530 $\sim$ 1565 nm, which is known as the C-band fiber amplifier.

Thus, a single EDFA can be used to amplify several channels simultaneously required for dense wavelength division multiplexing (DWDM). EDFAs are new tools that system planners now almost routinely use while designing high capacity optical networks. Practical EDFAs with output power of around 100 mW (20 dBm), 30 dB small signal gain, and a noise figure of < 5 dB are available commercially. We may note that core diameter of an EDF is typically smaller (almost half) of the standard single-mode fibers like SMF-28 and require special program(s) in a fiber splice machine to achieve low-loss splice of these special fibers with signal carrying standard fibers like SMF-28. Further, it could be seen from Fig. 4 that an integral component of an EDFA is a fused fiber coupler, which multiplexes 980 nm pump and 1550 nm band of signal wavelengths at the input of the EDF. In order for the fiber
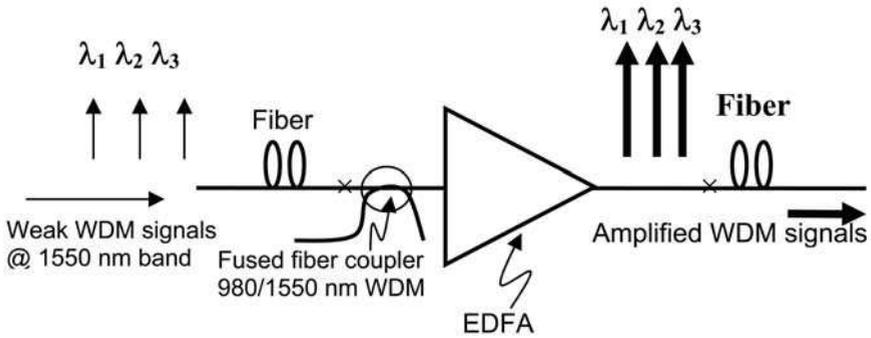
Fig. 4. Schematic of an EDFA in which 980 (or 1480) nm wavelength is used as a pump, which creates population inversion in Er^{+3} ions in the EDF and the weak WDM signals at the 1550 nm band get amplified as it propagates through the population inverted EDF
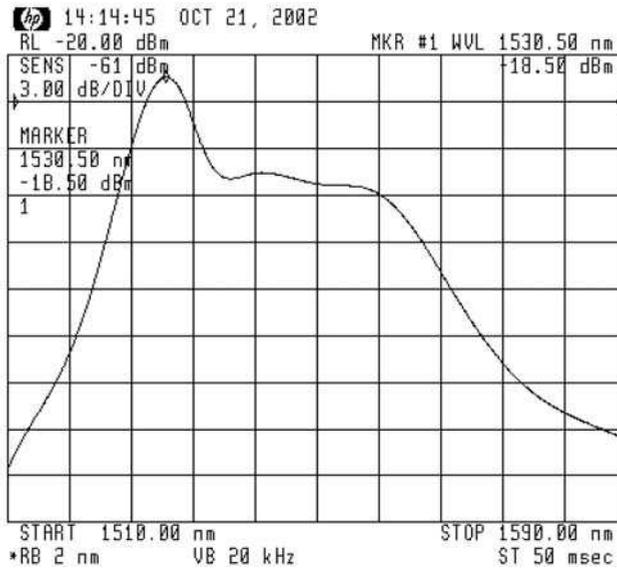

Fig. 5. Measured ASE spectrum (power vs wavelength) of an EDF as an example

used to configure such a multiplexer to be single moded at both the pump and signal wavelengths, λ_{ce} of the fiber should be < 980 nm. This led to development of special single-mode fibers known as SMF 980™ and Flexcor™ fibers, both being registered trademark of two different companies. Figure 5 shows typical amplified spontaneous emission (ASE) spectrum of an EDF when pumped with a diode laser at 980 nm. It could be seen from the figure that the spectrum is non-uniform, this caharacteristic in conjunction with the saturation effects of EDFAs cause increase in signal power levels and decrease in the optical signal-to-noise ratio (OSNR) to unacceptable values in systems consisting of cascaded chains of EDFAs [Srivastava & Sun, 2006]. These features could limit the usable bandwidth of EDFAs and hence the amount of data transmission by the system. Accordingly various

schemes of gain equalizing filters (GEF) such as Mach-Zehnder filter [Pan et al, 1995], acousto-optic filter [Kim et al, 1998], long-period fiber-grating [Vengsarkar et al, 1996], fiber-loop mirror [Li et al, 2001; Kumar et al, 2005], side-polished fiber based filter [Varshney et al, 2007] and so on have evolved in the literature. However, in the design of certain special networks like a metro network, one of the major drivers is low installation cost in addition to achieving low maintenance/repair costs. Naturally one of the routes to achieve these objectives would be to use fewer components in the network. Use of an intrinsically gain flattened EDFA would cut down the cost on the GEF head. This motivated some investigators [e.g., Nagaraju et al, 2009] to investigate design of an inherently gain flattened EDFA by exploiting a wavelength filtering mechanism inherent in a co-axial dual-core fiber design scheme. An example of the design of such a gain-flattened EDFA is shown in Fig. 6, which was based on a highly asymmetric dual-core concentric fiber design (see Fig. 6), whose inner core was only partially doped with erbium [Nagaraju et al, 2009]. Refractive index profile (RIP) of the designed inherently gain flattened EDFA and the RIP of the corresponding fabricated preform are shown in Fig. 6(a) and Fig. 6(b), respectively; r_d refers to ER^{+3} doping radius. The RIP was measured using a fiber analyzer. The so realized RIP was close to the designed one except for small profile perturbations typical in fibers fabricated by the MCVD process. Figure 7 shows the measured gain and noise figure as a
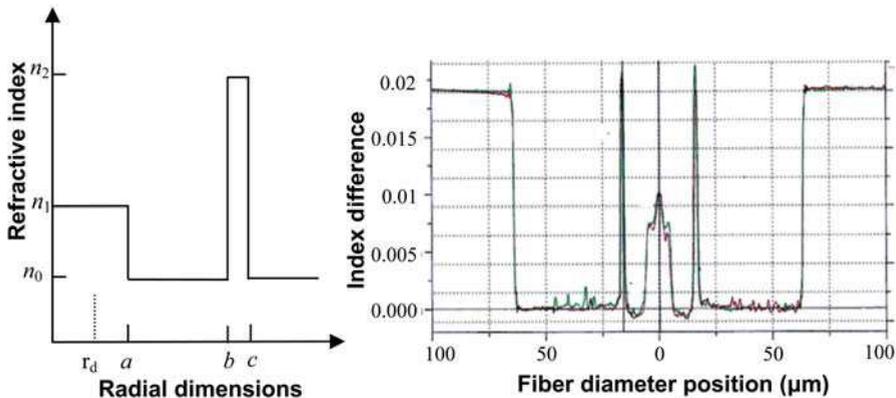

Fig. 6. a) Schematic of the theoretically designed refractive index profile of an inherently gain-flattened EDFA; b) Corresponding refractive index profile of the fabricated fiber preform (After Nagaraju et al, 2009; ©2009 Elsevier Press)

function of wavelength for the fabricated coaxial fiber; some improvements in the noise figure at longer wavelengths could be seen due to the increased overlap between the pump and the signal modes at longer wavelengths. Gain variation across the C-band was found to be more than the designed one, which is attributable to small variations in the fabricated fiber RIP parameters from the one that was designed. A very precise comparison is, in any case, difficult due to lack of sufficient precision inherent in measurement instruments for estimating various parameters of the fiber RIP and the dopant level. Phase-resonant optical coupling between the inner low index contrast core and the outer high index contrast narrow ring that surrounds the inner core was so tailored through optimization of its refractive index profile parameters that the longer wavelengths within the C-band experience relatively higher amplification compared to the shorter wavelengths
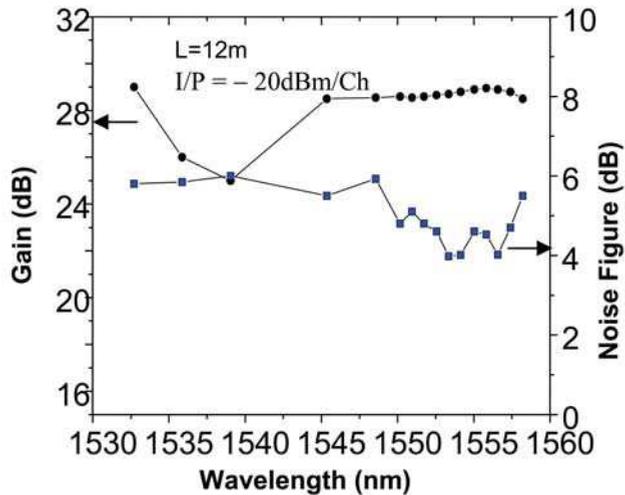
Fig. 7. Experimental results for measured gain (•) and noise figure (■) with wavelength on a 12 m long fabricated EDF (After Nagaraju et al, 2009; ©2009 Elsevier Press)

thereby reducing the difference in the well-known tilt in the gains between the shorter and longer wavelength regions. The fabricated EDFA exhibited a median gain ≥ 28 dB (gain excursion below ± 2.2 dB within the C-band) when 16 simultaneous standard signal channels were launched by keeping the I/P level for each at –20 dBm/channel. We may mention that another variety of EDFA is known as L-band EDFA, L standing for long wavelength band (1570 ~ 1610 nm) [Sun et al, 1997]. With suitable optimization of EDFAs, C-band and L-band amplifiers could be used as two discrete amplifiers to simultaneously amplify 160 signal wavelength channels by separating the transmission of two bands of weak signals for amplification by these amplifiers.

In addition to EDFA, another kind of fiber amplifiers that is commonly used is known as Raman fiber amplifiers (RFA). One of the nonlinear scattering processes namely, stimulated Raman scattering (SRS) is responsible for Raman amplification, which is quite broadband (up to 40 THz) with a broad peak appearing near 13.2 THz in bulk silica [Agrawal, 2007]. Classically this scattering process is described as an inelastic scattering process in which frequency of a propagating pump light beam of energy $\hbar\omega_P$ in a molecular medium shifts to a lower frequency i.e. suffers red shift to generate lower energy photon of energy $\hbar\omega_S$, which is determined by the molecular vibrational levels of the medium, in this case the doped silica fiber, according to the well known fundamental process known as the Raman effect. Without going in to the details, quantum mechanically it can be shown that the process leads to an amplification of a co-propagating signal as long as the frequency difference $\omega_P - \omega_S$ lies within the bandwidth of the Raman gain spectrum [Agrawal, 2007]. The most important parameter that characterizes the amplification process in a RFA is known as the Raman gain efficiency (C_R), defined as the ratio of coefficient (γ_R) to A_{eff} of a fiber. Figure 8 depicts a plot of C_R as a function of the difference $\omega_P - \omega_S$ in THz for three different variety of specialty fibers: NZDSF (A_{eff} ~ 55 μm^2), super large area special fiber (SLA of A_{eff} ~ 105 μm^2), and a dispersion compensating fiber (DCF of A_{eff} ~ 15 μm^2); pump wavelength was 1.45 μm and signal wavelength was ~ 1.55 μm [Bromage, 2004]. It can be seen that C_R is

largest in the case of DCF, which could be attributed to its A_{eff} that was the least and also it had a high Germania content compared to other two fiber varieties. Difference in the peak value of the Raman gain curve could be attributed to difference in A_{eff} and degree of overlap between the pump and the signal transverse modes [Urquhart & Laybourn, 1985; Bromage, 2004]. It is known that GeO_2 molecules exhibit larger peak gain (than silica) near 13.1 THz [15]. Dispersion compensating fibers, which represent one class of specialty fibers, are described in the next section; these are typically characterized with large Δ (typically ~ 2%) and small A_{eff}. In view of the large Raman gain exhibited by a typical DCF, these are often used as RFA. In certain DWDM systems, EDFA as well as RFA are used as a hybrid broadband amplifier for DWDM signals.
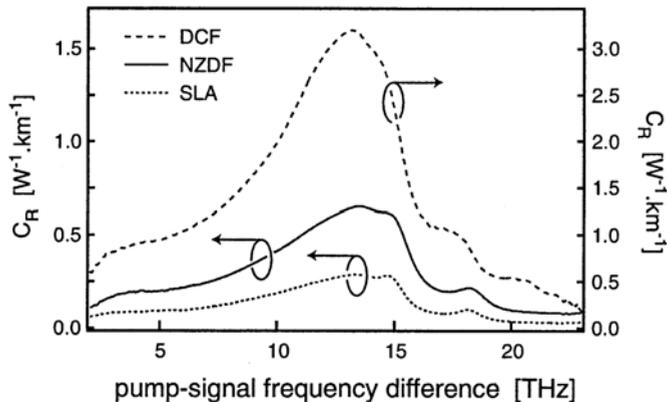
Fig. 8. Mesured C_R for three different variety of germanosilicate fibers having different 1550 nm A_{eff} and each pumped with 1450 nm diode laser (After Bromage, 2004; ©2004 IEEE).

3.2 Dispersion compensating fibers

To counter potentially detrimental nonlinear propagation effects in a DWDM link since a finite (albeit low) D is deliberately kept in NZDSF fibers, signals would accumulate dispersion between EDFA sites! Assuming a D of 2 ps/(nm.km), though a fiber length of about 500 km could be acceptable @ 10 Gbit/s before requiring correction for dispersion, @ 40 Gbit/s corresponding un-repeatered span would hardly extend to 50 km [see Eq. (2)]. The problem is more severe in G.652 fibers for which @ 2.5 Gbit/s though a link length of about 1000 km would be feasible at the 1550 nm window, if the bit rate is increased to 10 Gbit/s, tolerable D in this case over 1000 km would be hardly ~ 1 ps/(nm.km)! Realization of this fact triggered development of some dispersion compensating schemes in mid-1990s, which could be integrated to a single-mode fiber optic link so that net dispersion of the link could be maintained/managed within desirable limits. Three major state-of-the-art fiber-based optical technologies available as options for dispersion management are: *dispersion compensating fibers* (DCF) [Ramachandran, 2007], *chirped fiber Bragg gratings* (CFBG) [Kashyap, 1999], and *high-order-mode* (HOM) *fiber* [Ramachandran, 2006].

In order to understand the logic behind dispersion compensation techniques, we consider the instantaneous frequency of the output pulse from a single-mode fiber, which is given by [Thyagarajan & Pal, 2007]

$$\omega(t) = \omega_c + 2\kappa\left(t - \frac{L}{v_g}\right) \tag{8}$$

where ω_c represents carrier frequency, the center of the pulse corresponds to $t = L/v_g$, where v_g is the group velocity, and κ is a parameter, which depends on $d^2\beta/d\lambda_0^2$. Accordingly the leading and trailing edges of the pulse correspond to $t < L/v_g$ and $t > L/v_g$, respectively. In the normal dispersion regime (where operating wavelength < λ_{ZD}) κ is positive, thus the leading edge of the pulse will be down-shifted i.e *red-shifted* in frequency while the trailing edge will be up-shifted i.e. *blue-shifted* in frequency with respect to the center frequency ω_c. The converse would be true if the signal pulse wavelength corresponds to the anomalous dispersion region (operating $\lambda > \lambda_{ZD}$) where κ is negative. Hence as the pulse broadens with propagation due to this variation in its group velocity with wavelength in a dispersive medium like single-mode fiber it also gets chirped. If we consider propagation of signal pulses through a G.652 fiber at the 1550 nm wavelength band at which its *D* is positive, it would exhibit *anomalous* dispersion. If this broadened temporal pulse were transmitted through a DCF, which exhibits *normal* dispersion (i.e. its dispersion coefficient *D* is negative) at this wavelength band, then the broadened pulse would get compressed with propagation through the DCF. Thus if the following condition is satisfied:

$$D_T L_T + D_c L_c = 0 \tag{9}$$

the dispersed pulse would recover back its original shape; subscripts *T* and *c* stand for the transmission fiber and the DCF. Consequently if a G.652 fiber as the transmission fiber is operated at the EDFA band, corresponding DCF must exhibit negative dispersion at this wavelength band $\Rightarrow$ its D_{WG} (negative in sign) must be large enough to be more than D_M in magnitude. Large negative D_{WG} is achievable through appropriate design tailoring of the refractive index profile of the fiber so that at the wavelengths of interest a large fraction of its modal power rapidly spreads into the cladding region for a small change in the propagating wavelength. The *first generation* DCFs relied on narrow core and large Δ (typically ≥ 2 %) fibers to achieve this task and hence necessarily involved relatively large insertion loss. Accordingly, a parameter named as figure of merit (FOM) is usually ascribed to any DCF defined through

$$\text{FOM} = \frac{-D_c}{\alpha_c} \tag{10}$$

These DCFs were targeted to compensate dispersion in G.652 fibers at a single wavelength and were characterized with a $D \sim -50$ to -100 ps/(nm.km) and a positive dispersion slope. Since DWDM links involve multi-channel transmission, it is imperative that ideally one would require a broadband DCF so that dispersion could be compensated for all the wavelength channels simultaneously. The key to realize a broadband DCF lies in designing a DCF, in which not only that *D* versus λ is negative at all those wavelengths in a DWDM stream, but also its dispersion slope is negative. Broadband dispersion compensation ability of a DCF is quantifiable through a parameter known as relative dispersion slope (*RDS*), which is defined through [Pal, 2006; Thyagarajan & Pal, 2007]

$$RDS = \frac{S_c}{D_c} \tag{11}$$

Values of *RDS* (nm-1) for well-known NZ-DSF's like LEAF™, TrueWave-RS™, and Teralight™ are 0.0202, 0.01, and 0.0073, respectively. Thus if a DCF is so designed that its *RDS* matches that of the transmission fiber then that DCF would ensure perfect compensation for all the signal wavelengths. Such DCFs are known as dispersion slope compensating fibers (DSCF). *RDS* for G.652 fibers at 1550 nm is about 0.00335 nm^{-1}. One recent dual-core DCF design, whose refractive index profile was similar to that shown in Fig. 6 with the difference that it had a high refractive contrast for the central core and lower refractive contrast for the outer wider ring core, had yielded the record for largest negative *D* (– 1800 ps/(nm.km) at 1558 nm) in a DCF. The two cores essentially function like a directional coupler. Since these two concentric fibers are significantly non-identical, through adjustments of index profile parameters their mode effective indices could be made equal at some desired wavelength called phase matching wavelength (λp), in which case the effective indices as well as modal field distributions of the normal modes of this dual core fiber exhibit rapid variations with λ around λp [Thyagarajan & Pal, 2007]. Further research in this direction has led to designs of dual-core DSCFs for broadband dispersion compensation in G.652 as well as G.655 fibers within various amplifier bands like S-, C- and L- bands [Pal & Pande, 2002; Pande & Pal, 2003]. Mode effective areas of dual core DSCFs could be designed to attain A_{eff}, which are comparable to that of the G.652 fiber ($\approx$ 70 - 80 μm²). The net residual dispersion spectra of a 100 km long G.652 fiber link along with so designed DSCFs (approximately in ratio of 10:1) at each of the amplifier band are shown in Fig. 9. It could be seen that residual average dispersion is well within $\pm$ 1 ps/(nm.km) within all the three amplifier bands.
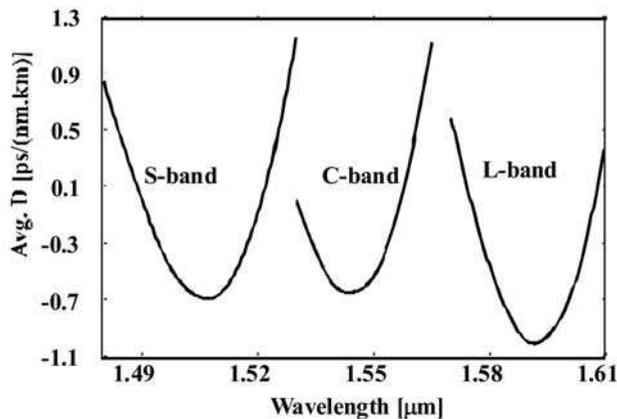

Fig. 9. Net residual dispersion at different amplifier bands of a dispersion compensated link design consisting of 100: 10 (in kms) of G.652 fiber and 10 km of a dual-core DSCFs (After Pal & Pande, 2004; ©2004 Elsevier Press).

3.3 Fibers for metro networks [Pal, 2006]
During the IT bubble burst, there has been a slowing down of business in optical communication due to the so-called huge fiber glut in the long haul networks (typically trans-oceanic). However, the gap between the demand and supply of bandwidth has been much less in the metro sector and in recent years metro optical networks have attracted a great deal of attention due to potentials for high growth. A metro network provides

generalized telecommunication services transporting any kind of signal from one point to another in a metro, usually running a couple of hundred kilometers in length. In transport, DWDM is the key enabling technology to expand the capacity of existing and new fiber cables without optical-to-electrical-to-optical conversions. Accordingly the network trend in the metro sector has been to move towards transparent rings, in which wavelength channels are routed past or dropped off at the nodes [Ryan, 2003]. Gigabit Ethernet is fast evolving as a universal protocol for optical packet switching. Thus, in addition to voice, video, and data a metro network should be able to support various protocols like Ethernet, fast Ethernet, and 10 Gbit/s Ethernet. DWDM in a metro environment is attractive in this regard for improved speed in provisioning due to possibility of allocating dynamic bandwidth on demand to customers and for better-cost efficiency in futuristic transparent networks running up to 200 km or more. Legacy metro networks relied heavily on directly modulated low-cost FP-lasers in contrast to the more expensive externally modulated DFB lasers. However directly modulated lasers are usually accompanied with a positive chirp, which could introduce severe pulse dispersion in the EDFA band if the transmission fiber is characterized with a positive D. The positive chirp-induced pulse broadening can be countered with a transmission fiber if it is characterized with normal dispersion (i.e. negative D) at the EDFA band. This is precisely the design philosophy followed by certain fiber manufacturers for deployment in a metro network e.g. MetroCor™ fiber of Corning Inc. For typical transmission distances encountered in a metro network, a DCF in the form of a standard SMF with positive D is used to compensate for dispersion in a MetroCor™ kind of fiber. However, due to a relatively low magnitude of D in a standard SMF, long lengths of it are required, which increase the overall loss budget and system cost. An alternative type of metro fiber has also been proposed and realized, which exhibits positive $D \sim 8$ ps/(nm.km) at 1550 nm [Ryan, 2002]. The argument in favor of such positive dispersion metro-fibers is that dispersion compensation could be achieved with readily available conventional DCFs of much shorter length(s) as compared to standard SMFs that would be necessary to compensate for the negative dispersion accumulated by the metro fibers [Ryan, 2002].

4. Microstructured Optical Fibers (MOF)

4.1 Discovery of the concept of photonic crystals
The state-of-the art in silica-based optical fiber technology could be described as
- Loss close to theoretical limit (0.14 dB/km)
- Dispersion could be tailored close to zero anywhere at a wavelength ≥ 1310 nm but not below 1200 nm unless fiber core is significantly reduced through tapering, for example [Birks et al, 2000]
- Minimum nonlinear impairments over distances ≥ 100 km
- High quality fiber amplifiers with low noise to compensate for whatever be the transmission loss; noise figure could be close to theoretical minimum of 3 dB
- Demonstration of hero experiments at transmission rates > terabit/s over a single fiber through modulation techniques like CSRZ-DQPSK and polarization mode division multiplexing.

With so much of development it appeared for a while that there was no further research scope for development of newer fibers. However it became increasingly evident in the early 1990s that there is a need to develop specialty fibers in which material loss is not a limiting factor and fibers in which nonlinearity and/ or dispersion could be tailored to achieve

propagation characteristics, which are otherwise impossible to achieve in conventional fibers. Two research groups – Optoelectronic Research Center in University of Southampton in UK (and soon after University of Bath) and MIT in USA exploited the concept of Photonic Crystals (PhC), which were proposed for the first time independently in two papers, that appeared simultaneously in the same issue of Physical Review Letters in 1987 [Yablonovich, 1987; John, 1987], to develop a completely new variety of specialty fibers broadly known as microstructured optical fibers. Yavlonovitch and John in their 1987 papers (coincidentally EDFA was also discovered in the same year!) showed independently that a lattice of dielectrics with right spacing and different optical properties could generate a photonic bandgap (analogous to electronic band gap in a semiconductor). A square lattice of periodic air holes in a higher index dielectric like silica shown in Fig. 10 could be cited as an example. They showed that wavelength scale structuring of such lattices in terms of refractive index features could be exploited as a powerful tool to modify their optical properties. Light wavelengths falling within the structure's characteristic band gap will not propagate i.e. would not be supported in that medium. If, however, a defect is created in the lattice (e.g. through removal of one hole at the center so that the region becomes a solid of same material as the rest of the medium) to disrupt its periodicity (akin to change in semiconductor properties by dopants), the same forbidden band of wavelengths could be supported and localized in that medium within the defect region. Thus if one were to extend this concept to a cylindrical geometry like a fiber, the defect region would mimic the core of an optical fiber with the surrounding 2D-periodic arrays of air holes in silica like PhC as forming a cladding of a lower average refractive index. This indeed formed the functional principle of "holey" type of MOFs. Due to strong interaction of the propagating light in the bandgap with the lattice, n_{eff} becomes a strong function of the propagating wavelength, which yields an additional functionality, which could be exploited to form a fiber that could function as an endlessly single-mode fiber over a huge bandwidth [Birks et al, 1997]. In view of this large bandwidth, holey fibers are usually not referred to as a photonic band gap structure while the other variety of microstructured fibers are often referred to as photonic bandgap guided fibers as described in the next sub-section.
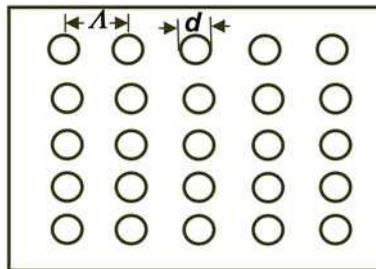

Fig. 10. A square lattice of periodic air holes in a higher index dielectric; Λ is the pitch and d is the diameter of the holes

4.2 Holey and photonic bandgap MOFs

Wavelength scale periodic refractive index features across its cross-section, which run throughout the length of the fiber, characterize MOFs [Monro, 2006]. These special fibers opened up a lot of application potentials not necessarily for telecom alone. In contrast to the

fundamental principle of waveguidance through total internal reflection in a conventional fiber, waveguidance in a MOF is decided by two different physical principles – *index* guided and *photonic bandgap* guided (PBG). In index guided MOFs like holey fibers (see Fig. 11), in which the central defect region formed by the absence of a hole yielding a material of refractive index same as the surrounding solid, light guidance in these MOFs could be explained by a *modified total internal reflection* due to the average refractive index created by the presence of PhC cladding consisting of 2D-periodic arrays of air holes in the silica matrix, which is lower than the central defect region. This average index of the cladding depends on the relative distribution of the modal power supported by the silica and air hole lattice, which vary with wavelength. As the wavelength decreases, more and more power gets concentrated within the high index region, the cladding index increases and effective relative refractive index difference between the core and the cladding decreases. As a result the normalized frequency remains relatively insensitive to wavelength. Accordingly, over a broad range of wavelengths the fiber functions as a single-mode fiber. In fact, if the ratio of air hole diameter to the pitch of crystal is kept below 0.45, the fiber remains endlessly single moded [Knight et al, 1996; Birks et al, 1997]. For larger d/Λ, it supports higher order modes as long as λ/Λ is < a critical value.
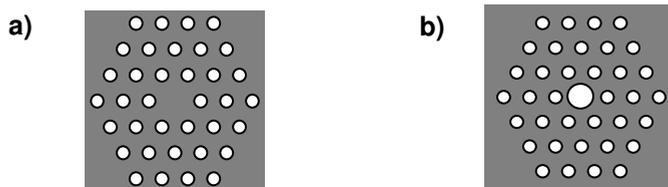
Fig. 11. Schematics of MOFs with white regions representing air or low index medium a) index guided holey type; b) Photonic bandgap guided fiber.

In contrast, in a photonic band gap guided MOF, the central defect region is of a lower refractive index (usually air), which forms the core; typically it is larger in diameter than the low index regions of the PhC cladding. The central core region could have a refractive index same as that of the low index region of the periodic cladding. Functionally light within the photonic bandgap is confined in the central lower index region due to multiple Bragg reflections from the air-silica dielectric interfaces, which add up in phase. Though periodicity is not essential in case of index-guided structures, periodicity is essential in case of PBG guided structures.

4.3 Dispersion tailored holey fibers

Availability of MOFs offered a huge design freedom to fiber designers because a designer could manipulate propagation effects in such a fiber through either or all of the parameters such as lattice pitch (Λ), air hole size (d) and shape, refractive index of the glass, pattern of the lattice, core size and refractive index. We depict some sample results based on use of the software CUDOS[*] (of University of Sydney, Australia). It is evident from Fig. 12 that D

---

[*] CUDOS is license free software for simulating index-guided MOFs that is available from University of Sydney, Australia.

becomes a stronger function of wavelength as pitch decreases for a fixed size of the hole and also for larger holes when pitch is kept fixed. Figure 13 depicts D versus wavelength for an index guided DCF, in which the air hole size of one of the outer rings has been reduced, thereby effectively functioning as an outer core of smaller index contrast. Its effective refractive index profile is analogus to that of a dual concentric core fiber discussed earlier in the section on DCF. Figure 13 representing its dispersion spectrum shows broadband DCF nature of such a structure when appropriately optimised. Our deeper studies on such a broadband DCF have revealed that D vs λ curve becomes flatter and confinement loss becomes smaller when the outer core i.e. the ring with smaller sized holes is nearer to the core. Dispersion slope of the designed DCF is ~ -3.7 ps/km.nm^2, and accordingly its RDS is 0.00357 nm^{-1}, which matches well with the RDS value for standard G.652 type of single-mode fibers (0.0036 nm^{-1}). Figure 14 depicts effect of varying d_2 on D vs λ curve for the dual core holey fiber of the kind shown on Fig. 13. The confinement loss was found to reduce from $\sim 10^3$ to $\sim 10^{-1}$ dB/m as the number of cladding rings increases from 5 to 8.
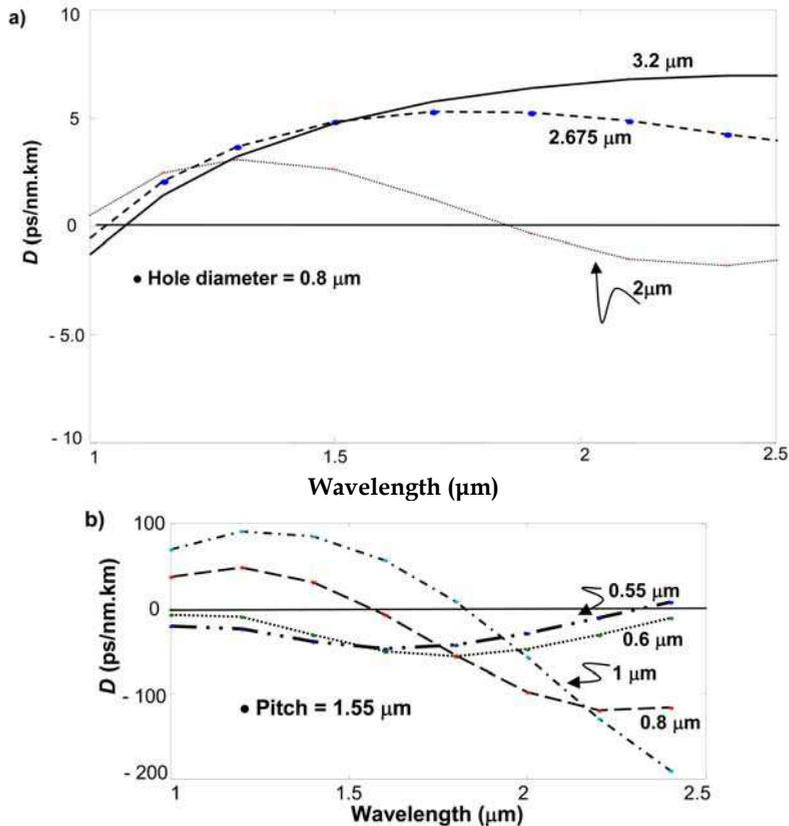
Fig. 12. Dispersion spectra in a holey fier having three cladding rings; a) for different pitch and constant hole diameter; b) foe different hole diameter and constant pitch [After Mehta, 2009]
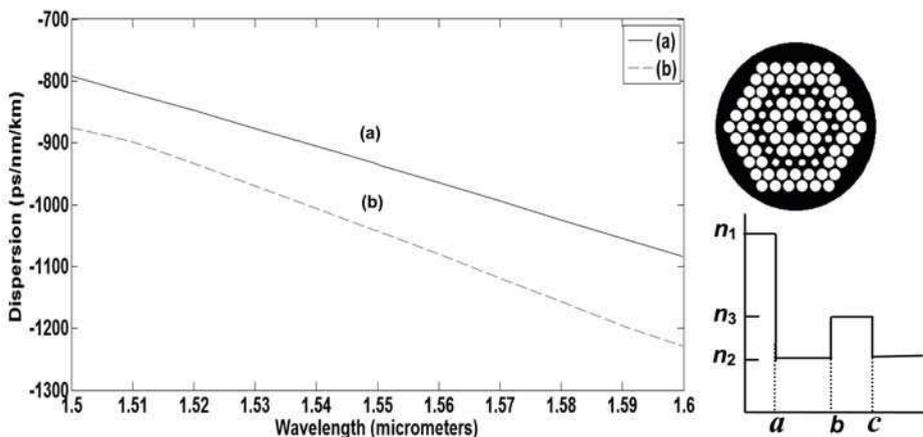
Fig. 13. Dispersion spectra of index guided DCF (shown on the side), whose pitch (Λ) is 0.8 μm and d_1/Λ = 0.85; a) for d_2= 0.58 μm, b) for d_2= 0.56 μm; d_1 corresponds to diameter for the bigger air holes in the cladding rings while d_2 ($<d_1$) correspond to diameter of the air holes in the third outer ring. Equivalent effective refractive index profile is also shown in the figure [After Mehta, 2009].
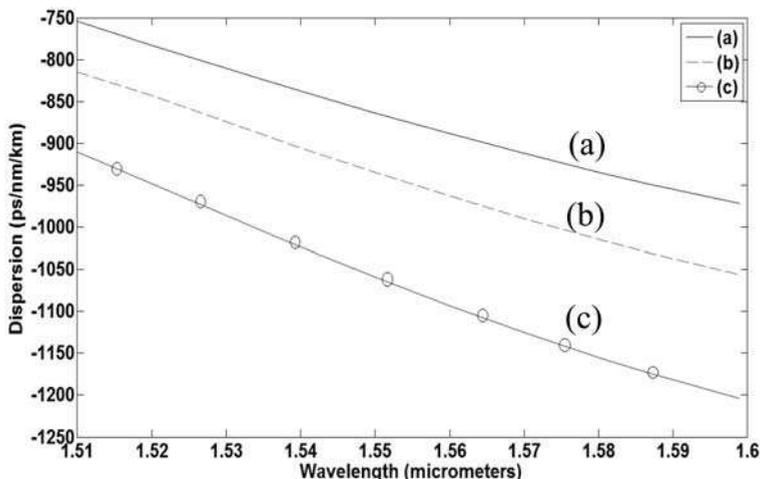

Fig. 14. Effect on dispersion spectrum for variation in d_1 while d_2 and pitch were kept fixed at 0.3 μm and 1 μm, respectively; (a) d_1 = 0.85 μm, (b) d_1 = 0.87 μm, (c) d_1 = 0.9 μm. [After Mehta, 2009]

Confinement loss is an important characteristic parameter of MOFs. It is defined as (Kuhlmey et al, 2002)

$$\text{Confinement loss (dB/m)} = \frac{20 \times 10^6}{\ln 10} \frac{2\pi}{\lambda} \text{Im}\left(n_{\text{eff}}\right) \tag{12}$$

where n_{eff} is effective index of the fiber mode.

4.4 Birefingent microstructured optical fiber

Birefringence could be easily generated in a MOF by increasing diameter of the holes adjacent to the core along one direction as shown in Fig. 15. Birefringence (B) is defined through Eq. (12). In Fig. 16, we depict sample of a typical variation of B with the ring

$$B = n_x - n_y = \frac{\lambda\left(\beta_x - \beta_y\right)}{2\pi} \tag{12}$$

location in which the diametrically opposite larger sized pair of holes on a specific ring in the cladding. It is apparent that birefringence reduces as the pair of diametrically opposite air holes is located farther away from the core of the holey fiber.
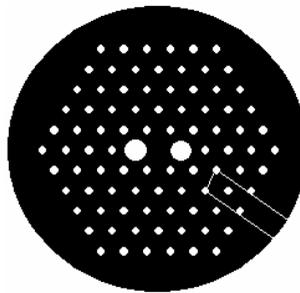
Fig. 15. Cross section of a sample birefringent index guided holey MOF
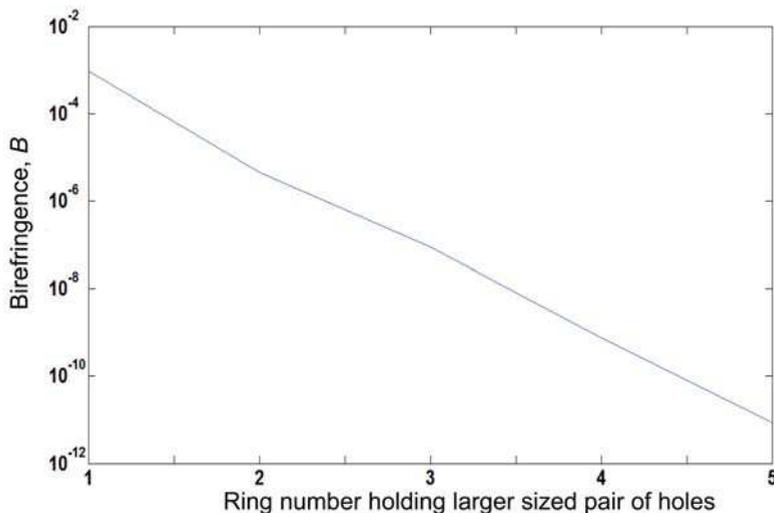
Fig. 16. Birefringence as a function of location of the larger sized pair of holes with respect to the core of the holey fiber [After Mehta, 2009]

5. One dimensional photonic bandgap fibers: Bragg fiber

5.1 Dispersion compensating Bragg fibers

Bragg fibers represent an 1D-PBG MOF, which was first proposed in 1978 [Yeh et al, 1978], almost 10 years before the concept of PhC emerged; although the authors missed out in identifying the inherent photonic band gap characteristic feature of these fibers. These fibers consist of a low-index central region (serving as the core) that is surrounded by concentric layers of alternate high and low refractive index materials. Although in the first proposal the refractive indexes of the cladding bilayers were assumed to be higher than that of the core (see Fig. 17), Bragg fibers could also be designed such that only one of the cladding bilayers has a refractive index higher than that of the core [Katagiri et al, 2004].
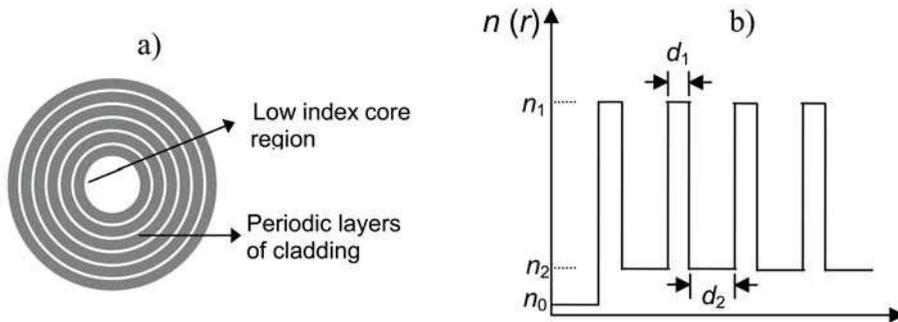
Fig. 17. a) Cross sectional view of a Bragg fiber; b) Corresponding refractive index profile

In either case, the refractive index periodicity in the cladding spawns a PBG. In mid-1980s, air-core Bragg fibers attracted some attention due to a possibility of guiding light in an air core, thereby offering the possibility of attaining a very low transmission loss [Doran & Blow, 1983]. With the emergence of the concept of PBGs in the context of photonic crystals there has been a resurgence of interest in air-core Bragg fibers as an alternative PBG fiber platform for a variety of applications. The first report on a solid silica-core Bragg fiber appeared in 2000 [Brechet et al, 2000], which aimed to achieve zero GVD at wavelengths shorter than conventional telecommunication wavelength windows; in addition, liquid-filled polymer-based Bragg fibers [Cox et al, 2006; Pone et al, 2006], and hollow/low-index core Bragg fibers [Argyros et al, 2006; Skorobogatiy, 2005] also attracted attention because they exhibit diverse propagation characteristics. Bragg fibers with relatively large refractive index difference between its core material and cladding layer materials could essentially be modeled like planar stacks of periodic thin films of alternating materials, similar to an interference filter [Dasgupta et al, 2006]. Inherently the Bragg fibers are leaky in nature due to its refractive index profile, however the loss can be minimized by appropriately choosing the cladding layer parameters. For a given number of cladding layers, the following *quarter-wave stack condition* minimizes the radiation loss of the TE modes supported by a Bragg fiber

$$k_0 n_1 d_1 = k_0 n_2 d_2 = m\pi/2 \qquad (19)$$

where n_1, n_2 and d_1, d_2 are the refractive indices and thickness of odd and even layers, respectively, k_0 is free space wave number at the operating wavelength, which is the central wavelength of the band gap that is characteristic of the Bragg fiber and the integer m (≥ 1)

represents order of the quarter wave stack condition. Satisfying this condition implies that round-trip optical phase accumulated from traversal through a pair of claddings is 2π. By choosing $m = 3$, design of a dispersion compensating Bragg fiber (DCBF) of extremely large figure of merit has been reported [Dasgupta et al, 2005]. Figure 18 depicts radiation loss and dispersion spectra of the designed air-core high index contrast Bragg fiber based on a polystyrene-tellurium (PS-Te) material system. It could be seen that this DCBF exhibits dispersion and radiation losses of −1245 ps/(nm.km) and 0.006 dB/km (with 20 cladding bi-layers), respectively, at 1550 nm. These values amount to an effective FOM of 200,000 ps/(nm.dB), which are 2 orders of magnitude larger than that of conventional DCFs. The average dispersion of the DCBF is −1800 ps/(nm.km) across the C-band of an EDFA, with an estimated average radiation loss of 0.1 dB/km.
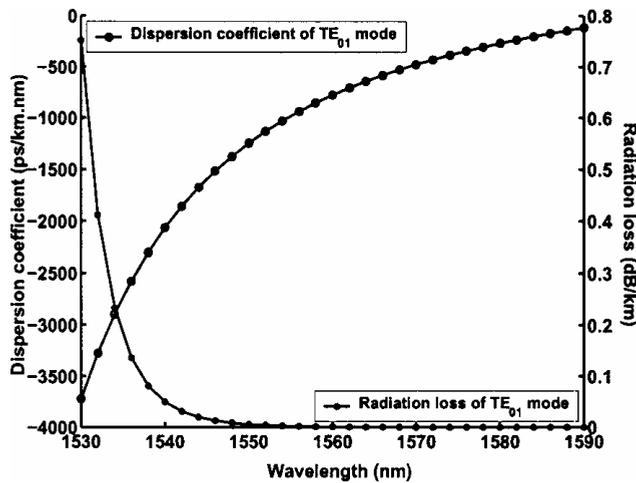
Fig. 18. Dispersion and radiation loss spectra of an air-core Bragg fiber-based DCF [After Dasgupta et al, 2005; ©2005 OSA]

5.2 Bragg fiber for metro networks

Exact modeling of Bragg fibers as reported in [Yeh et al, 1978] was extremely computation intensive because of the large number of material interfaces involved. However, a semi-asymptotic matrix approach involving much less complexity and computational time has been reported in [Xu et al, 2003], according to which the field in the first few of the inner cladding layers are assumed to be exact Bessel solutions while the field in the rest of the outer layers is assumed to be describable by the asymptotic form of Bessel functions. The Bloch theorem is then applied to set up the eigen value equation, solutions of which give the propagation constants of the guided modes. This formalism has been applied to design an air core metro centric Bragg fiber [Pal et al, 2005]. Figure 19 shows the dispersion spectrum of the lowest order TE mode of such a metro-centric Bragg fiber. Its dispersion characteristics are very close to that of the metro fiber of AlcaLuc, average dispersion of the fiber across the C band being 10.4 ps/(nm.km) with a dispersion slope of 0.17 ps/(nm^2.km) at 1550 nm. This should enable a dispersion-limited fiber reach before dispersion compensation is required of ~ 96 km in the C band at 10 Gbits/s, assuming dispersion power penalty of 1 dB. Its average dispersion across the L-band was 15.9 ps/(nm.km) with

a dispersion slope of 0.09 ps/(nm².km) at 1590 nm. Inserting a conventional dispersion compensating fiber or another Bragg fiber-based dispersion compensator discussed in the previous section can easily compensate the accumulated positive dispersion of this NZDSF in a metro-like network system. The strong confinement of the TE_{01} mode within the air-core allows the material-related losses in the cladding to be ignored at the design stage as compared to the radiation loss. The average radiation loss of the TE_{01} mode across the C band was estimated to be only 0.03 dB/km while it was nearly an order of magnitude lower across the L band. To achieve efficient optical coupling, this Bragg fiber, which had a core diameter of ~ 10 μm, can be tapered to attain significant modal overlap between its TE_{01} mode and the LP_{01} mode of the SMF-28 single-mode fiber pigtail of a laser diode. Additionally, the air-core of the Bragg fiber enhances the threshold for optical nonlinearity while simultaneously allowing a large mode effective area as compared to conventional fibers - both these features are attractive for large power throughput with low sensitivity to detrimental nonlinear effects. Large power throughput serves to offset the signal distribution losses at the nodes of a typical metro and/ regional network rings, which is advantageous from the point of view of power budgeting options. Such a metro fiber, if realized should allow a fiber span length of ~ 100 km without requiring any dispersion compensating device and amplifier. These features, to a large extent, satisfy the required features like reduced installation and operational costs, and complexity of a metropolitan network.
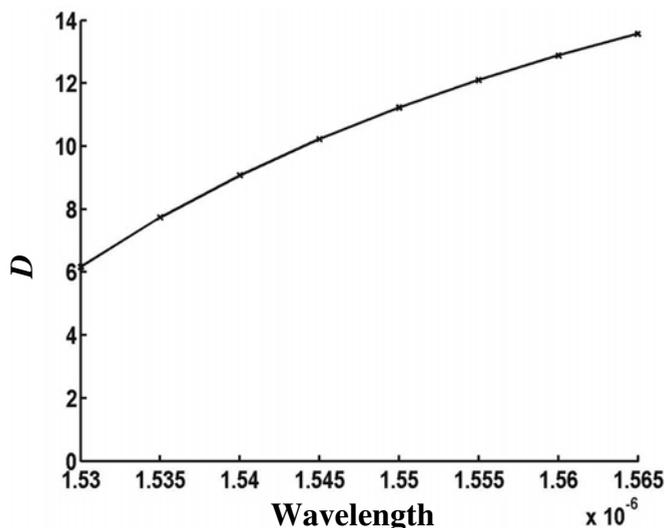

Fig. 19. Dispersion spectrum for the TE_{01} mode of a positive dispersion flattened air core Metro centric Bragg fiber [After Pal et al, 2005 ; ©2005 OSA]

5.3 Nonlinear spectral broadening in solid core Bragg fibers

Solid core Bragg fibers could be designed to have very small (~ 3 μm²) or very large mode area (~ 500 μm²). The first report on realization of a solid core Bragg fiber was reported in [Brechet et al, 2000]. Solid core Bragg fibers are attractive from fabrication point of view and also for investigating nonlinear effects in such fibers. As in index guided and photonic

bandgap guided MOFs fibers, zero dispersion in a Bragg fiber could be tailored to wavelengths below 1200 nm. An important additional advantage offered by a solid core Bragg fibers is that it could be fabricated by the widely well-known and mature process of modified chemical vapor deposition (MCVD) technology unlike the complex process involved in fabricating other varieties of MOFs. We have studied the phenomenon of supercontinuum generation centered at 1.05 μm in a solid core dispersion decreasing Bragg fiber (DDBF) [Pal et al, 2006; Dasgupta et al, 2007]. Since a silica-based solid core fiber amenable to fabrication by the MCVD technology would be a low index contrast fiber, evolution of a short high power pulse in a silica core Bragg fiber having 10 bi-layers of cladding was designed by modeling it through a matrix method applicable to LP modes of an optical fiber [Pal et al, 2006]. By simulating the propagation of different order soliton pulses, we observed that the shortest distance at which such a pulse is maximally compressed is $\sim z_0/(N-1)$, where z_0 is the soliton period, and N is the whole integral value for $N \geq 2$. Beyond this propagation distance, the pulse begins to break up, and the corresponding frequency spectrum does not exhibit any further broadening. Pulse evolution with propagation in the frequency domain as modeled through solution of the nonlinear Schroedinger equation [Agrawal, 2007] and taking in to consideration higher order group velocity dispersion effects. Maximum broadening of the pulse in the frequency domain was found to occur in a dispersion decreasing fiber (through up-taper along its length) of length ~ 70 cm. The nonlinearity induced broadening of the pulse as a supercontinuum pulse at the output of the dispersion decreasing Bragg fiber is shown in Fig. 20; it could be seen that the 25 BW of the output pulse is ~ 152 nm. It could be broadened further but at the expense of worsening of the flatness of the spectrum. Still broader spectrum would be possible if a lower dispersion slope Bragg fiber could be designed. More recently experimental demonstration of super continuum light from a solid core Bragg fiber fabricated through the MCVD method has been reported [Bookey et al, 2008] (as shown in Fig. 21).
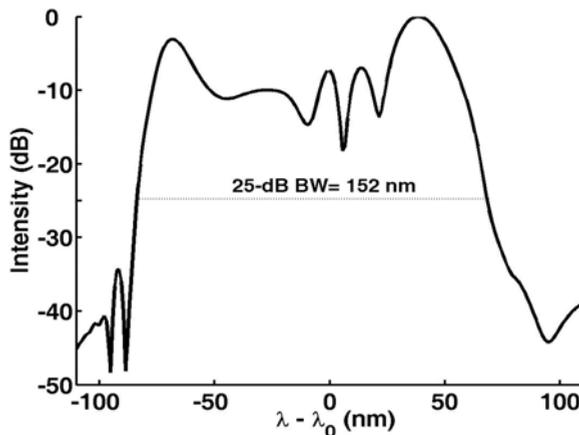

Fig. 20. Simulations demonstrating broadened frequency spectrum achieved through a dispersion decreasing solid core Bragg fiber for a 100 fs input pulse of peak power 4 kW [Calculations courtesy Dasgupta, 2006]
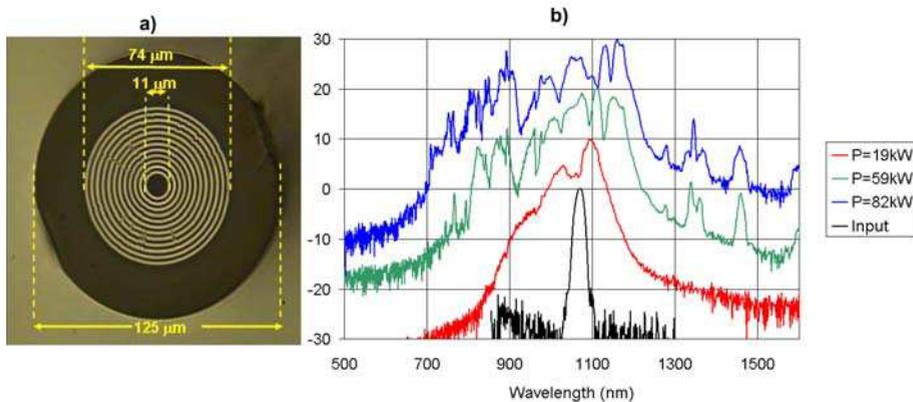
Fig. 21. a) Optical micrograph of the cross section of a solid core Bragg fiber fabricated through MCVD technology; b) Nonlinear spectral broadening in 3 cm of this Bragg fiber showing the input spectrum and for 19 kW, 59 kW, and 82 kW of launched peak powers from an optical parametric amplifier (OPA). OPA was tuned to 1067 nm and FWHM of the launched pulse was 120 fs (After Bookey et al, 2009; ©2009 OSA).

6. Conclusion

In this chapter we have attempted to provide a unified summary description of the most important propagation characteristics of an optical fiber followed by discussion on several variety of special fibers for realizing fiber amplifiers, dispersion compensating fibers, microstructured optical fibers, and so on. Even though huge progress has been made on development of optical fibers for telecom application, a need for developing special fibers, not necessarily for telecom alone, has arisen. This chapter was an effort to describe some of these special fibers. Detailed discussions are given on our own work related to inherently gain-flattened EDFA, DCFs of large mode effective area, index-guided MOF and Bragg fibers for realizing dispersion compensation, for metro network centric applications, and for generating super continuum light.

7. Acknowledgement

8. References

Agrawal, G. P. (2007), *Nonlinear Fiber Optics*, Fourth edition, Academic Press, San Diego.

Agrawal, G. P. (2006a), Fiber optic Raman amplifiers in *Guided Wave Optical Components and Devices: basics, Technology, and Applications*, B. P. Pal (Ed.), pp. 1-25, Elsevier Academic Press, Burlington & San Diego.

Argyros, A., Eijkelenborg, M. V., Large, M. and Basset, I. (2006), Hollow core microstructure polymer optical fiber, *Opt. Lett.*, Vol. 31, pp. 172-174.

Auguste, J. L., Jindal, R., Blondy, J. M., Clapeau, M., Marcou, J., Dussardier, B., Monnom, G., Ostrowsky, D. B., Pal, B. P. and Thyagarajan K. (2000), -1800 ps/(nm.km) chromatic dispersion at 1.55 µm in a dual-core fiber, *Electron. Lett.* Vol. 36, pp. 1689-1691.

Birks, T. A., Knight, J. C., and Russel, P. St. J. (1997), Endlessly single-mode photonic crystal fiber, *Opt. Lett.*, Vol. 22, pp. 961-963.

Birks, T. A., Wadsworth W. A., and Russel, P. St. J. (2000) Supercontinuum generation in tapered fibers, *Opt. Lett.* Vol. 25, pp. 1415-1417.

Bookey H. T., Dasgupta, S., Bezawada, N., Pal, B. P., Sysoliatin, A., McCarthy, J. E., Salganskii, M., Khopin, V., and Kar, A. K. (2009), Experimental demonstration of spectral broadening in an all-silica Bragg fiber, *Opt. Exp.* Vol. 17, pp. 17130-17135.

Brechet, F., Roy, P., Marcou, J. and Pagnoux, D. (2000), Single-mode propagation in to depressed-core-index photonic bandgap fiber designed for zero-dispersion propagation at short wavelength, *Electron. Lett.*, Vol. 36, pp. 514-515.

Bromage, J. (2004), Raman amplification for fiber communication systems, *IEEE J. lightwave Tech.*, Vol. 22, pp. 79-93.

Cox, F.M., Argyros, A. and Large, M .C. J. (2006), Liquid-filled hollow core microstructured polymer optical fiber, *Opt. Exp.*, Vol. 14, pp. 4135-4140.

Dasgupta, S., Pal, B. P. and Shenoy, M. R. (2005), Design of dispersion compensating Bragg fiber with ultrahigh figure of merit, *Opt. Lett.*, Vol. 30, pp. 1917-1919.

Dasgupta, S. (2006), Personal Communication.

Dasgupta, S., Pal, B. P. and Shenoy, M. R. (2006), Photonic bandgap guided Bragg fibers in *Guided Wave Optical Components and Devices: basics, Technology, and Applications*, B. P. Pal (Ed.), pp. 1-25, Elsevier Academic Press, Burlington & San Diego.

Dasgupta, S., Pal, B. P. and Shenoy, M. R. (2007), Nonlinear spectral broadening in solid core Bragg fibers, *IEEE J. Lightwave Tech.*, Vol. 25, pp. 2475-2481.

Doran, N. J. and Blow, K. J. (1983), Cylindrical Bragg fibers: a design and feasibility study for optical communications, *IEEE J. Lightwave Tech.*, Vol. LT-1, pp. 588-590.

Ebendorff-Heidepriem, H., Petropoulos, P., Asimakis, S., Finazzi, V., Moore, R. C., Frampton, K., Koizumi, F., Richardson, D. J. and Monro, T. M. (2004), Bismuth glass holey fibers with high nonlinearity, *Opt. Exp.*, Vol. 12, pp. 5082-5087.

Ghatak, A. and Thyagarajan, K. (1998), *Introduction to Fiber Optics*, Cambridge University Press, Cambridge.

John, S. (1987), Strong localization of photons in certain disordered dielectric superlattices, *Phys. Rev. Letts.*, Vol. 58, pp. 2486-2489.

Johnson, S. G., Ibanescu, M., Skorobogatiy, Weisberg, O., Engeness, T. D., Solgacic, M., Jacobs, S. A. and Joannopoulos, J. D. (2001), Low loss asymptotically single-mode propagation in large core omniguide fibers, *Opt. Exp.*, Vol. 9, pp. 748-779.

Kartapoulos, S. K. (2000), *Introduction to DWDM Technologies*, SPIE Press, Bellingham, Washington & IEEE Press, Piscataway, NJ.

Kashyap, R. (1999), *Fiber Bragg Gratings*, Academic Press, San Diego.

Katagiri, T., Matsuura, Y. and Miyagi, M. (2004), Photonic bandgap fiber with a silica core and multiplayer dielectric cladding, *Opt. Lett.*, Vol. 29, pp. 557-559.

Kim, H. S., Yun, S. H., Kim, H. K., Park, N., and Kim, B. Y. (1998), Actively gain-flattened erbium-doped fiber amplifier over 35 nm by using all-fiber acousto-optic tunable filters, *IEEE Photon. Tech. Lett.*, Vol. 10, pp. 790-792..

Knight, J. C., Birks, T. A., Russel, P. St. J., and Atkin, D. M. (1996), All-silica single-mode optical fiber with photonic crystal cladding, *Opt. Lett.*, Vol. 21, pp. 1547- 1549.

Kuhlmey, B. T., White, T. P., Renversez, G., Maystre, D., Botten, L. C., de Sterke, C. M., and McPhedran, R. C., 2002, Multipole method for microstructured optical fibers,.II. Formulation, *J. Opt. Soc. Am. B*, Vol.19, pp. 2331-2340.

Kumar, N., Shenoy, M.R., Pal, B.P. (2005), A standard fiber-based loop mirror as a gain-flattening filter for erbium-doped fiber amplifiers, *IEEE Photon. Tech. Lett.*, Vol. 17, pp. 2056-2058.

Li, S., Chiang, K. S., Gambling, W. A. (2001), Gain flattening of an erbium-dped fiber amplifier using a high-birefringence loop mirror, *IEEE Photon. Technol. Lett.*, Vol. 13, pp. 942-944.

Li, T. (1995), The impact of optical amplifiers on long-distance lightwave communications, *Proc. IEEE*, Vol. 81, pp. 1568-1579.

Mehta, M. (2009), M.Tech. (Optoelectronics and Optical Communication) dissertation *Studies on Microstructured Optical Fibers*, IIT Delhi.

Mears, R.J., Reekie, L., Poole, S. B. and Payne, D. N. (1986), Low-threshold tunable cw and Q-switched fiber laser operating at 1.55 μm, *Electron. Lett.*, Vol. 22, pp. 159-160.

Mears, R. J., Reekie, L., Jauncy, I. M. and Payne, D. N., (1987), Low-noise fiber amplifier operating at 1.54 μm, *Electron. Lett.*, Vol. 23, pp. 1026-1027.

Miya, T., Terunume, Y., Hosaka, T. and Miyashita, T. (1979), An ultimate low-loss single-mode fiber at 1.55 μm, *Electron. Lett.*, Vol. 5, pp. 106-108.

Monro, T. M. (2006), Microstructured Optical fibers in *Guided Wave Optical Components and Devices: basics, Technology, and Applications*], B. P. Pal (Ed.), pp. 1-25 Elsevier Academic Press, Burlington & San Diego.

Nagaraju, B., Paul, M. C., Pal, M., Pal, A., Varsheny, R. K., Pal, B. P., Bhadra, S. K., Monnom, G. and Bernard, D. (2009), Design and fabrication of an intrinsically gain flattened Erbium doped fiber amplifier, *Opt. Comm.*, Vol. 282, pp. 2335-2338.

Okuno, T., Onishi, M., Kashiwada, T., Ishikawa, S. and Nishimura, M. (1999), Silica-based functional fibers with enhanced nonlinearity and confinement loss trade-offs, *IEEE J. Select. Top. Quantum Electron.*, Vol. 5, pp. 1385-1391.

Pal, B. P. (1995), Optical transmission in *Perspective in Optoelectronics*, S. S. Jha (Ed.), pp. 195-297, World Scientific, Singapore.

Pal, B. P. (2006), Optical fibers for broadband lightwave communication: evolutionary trends in designs in *Guided Wave Optical Components and Devices: basics, Technology, and Applications*, B. P. Pal (Ed.), pp. 1-25, Elsevier Academic Press, Burlington & San Diego.

Pal, B. P. and Pande, K. (2002), Optimization of a dual-core dispersion slope compensating fiber for DWDM transmission in the 1480-1610 nm band through G.652 single-mode fibers, *Opt. Comm.*, Vol. 201, pp. 335-344.

Pal, B. P., Dasgupta, S. and Shenoy, M. R. (2005), Bragg fiber designs for transparent metro networks, *Opt. Exp.*, Vol. 13, pp. 621-626.

Pal, B.P., Dasgupta, S. and Shenoy, M. R. (2006), Supercontinuum generation in a Bragg fiber: a novel proposal, *Optoelectron. Letts.*, Vol. 5, pp. 342-344.

Pan, J.Y., Ali, M. A., Elrefaie, A. F., and Wagner, R. E. (1995), Multi-wavelength fiber amplifier cascades with equalization employing Mach-Zehnder optical filter, *IEEE Photon. Technol. Lett.*, Vol. 7, pp. 1501-1503.

Pande, K. and Pal, B. P. (2003), Design optimization of a dual-core dispersion compensating fiber with high figure of merit and a large mode effective area for dense wavelength division multiplexed transmission through standard G.655 fibers, *App. Opt.*, Vol. 42, pp. 3785-3791.

Payne, D. N. and Gambling, W. A. (1975), Zero material dispersion in optical fibers, *Electron. Lett.*, Vol. 11, pp. 176-178.

Pone, P., Dubois, C., Guo, N., Gao, Y., Dupuis, A., Boismenu, F., Lacroix, S. and Skorobogatiy, M. (2006), Drawing of the hollow all-polymer Bragg fibers, *Opt. Exp.*, Vol. 14, pp. 5838-5852.

Ramachandran, S. (Ed.) (2007), *Fiber-based Dispersion Compensation*, Springer-Verlag, Berlin.

Ramachandran, S. (2006), Dispersion-tailored higher order mode fibers for in-fiber photonic devices in *Guided Wave Optical Components and Devices: Basics, Technology, and Applications*], B. P. Pal (Ed.), pp. 291-310, Elsevier Academic Press, Burlington & San Diego.

Ryan, J. (2002), Fiber considerations for metropolitan networks, *Alcatel Telecom. Rev.*, Vol. 1, pp. 52-56.

Skorobogatiy, M. (2005), Efficient ant-guiding of TE and TM polarizations in low index core waveguides without the need of omnidirectional refelector, *Opt. Lett.*, Vol. 30, pp. 2991-2993.

Sun, Y, Sulhoff, J. W., Srivastava, A., Zysking, J. L., Srasser, T. A., Pedrazzani, J. R., Wolf, C., Zhou, J., Judkins, J. B., Espindola, R. P., and Vengsarkar, A. M. (1997), 80 nm ultra wideband erbium doped silica fiber amplifier, *Electron. Lett.*, Vol. 33, pp. 1965-1967.

Srivastava, A. and Sun, Y. (2006), Erbium-doped fiber amplifiers for dynamic optical networks in *Guided Wave Optical Components and Devices: Basics, Technology, and Applications*], B. P. Pal (Ed.), pp. 181-204, Elsevier Academic Press, Burlington & San Diego.

Thyagarajan, K., Diggavi, S., Taneja, A. and Ghatak, A. K. (1991), A simple numerical technique for the analysis of cylindrically symmetric refractive index profile optical fiber, *Appl. Opt.*, Vol. 30, pp. 3877-3879.

Thyagarajan, K. and Pal, B. P. (2007), Modeling dispersion in optical fibers: applications to dispersion tailoring and dispersion compensation in *Optical Fiber Communication Reports*, Ramachandran, S. (Ed.), Vol. 4, pp. 173–213, Springer-Verlag, Berlin.

Urquhart, W. P. and Laybourn, P. J. (1985), Effective core area for stimulated Raman scattering in single-mode optical fibers, *Proc. Inst. Elect. Eng.*, Vol. 132, pp. 201–204.

Xu, Y., Yariv, A., Fleming, J. G. and Lin S. Y. (2003), Asymptotic analysis of silicon based Bragg fibers, *Opt. Exp.*, Vol. 11, pp. 1039-1049.

Varshney, R. K., Nagaraju, B., Singh, A., Pal, B. P., and Kar, A. K. (2007), Design and Realization of an All-Fiber Broadband Tunable Gain Equalization Filter for DWDM Signals, *Opt. Exp.*, Vol. 15, pp. 13519-13530.

Vengsarkar, A. M., Lemaire, P.J., Judkins, J. B., Bhatia, V., Erdogan, T., Sipe, J. E. (1996), Long period fiber gratings as band rejection filters, *IEEE J. Lightwave Tech.*, Vol. 14, pp. 58-65.

Yablonovitch, E. (1987), Inhibited spontaneous emission in solid-state physics and electronics, *Phys. Rev. Letts.*, Vol. 58, pp. 2059-2062.

Yeh, P., Yariv, A. and Marom, E. (1978), Theory of Bragg fiber, *J. Opt. Soc. Am.*, Vol. 68, pp. 1196-1201.
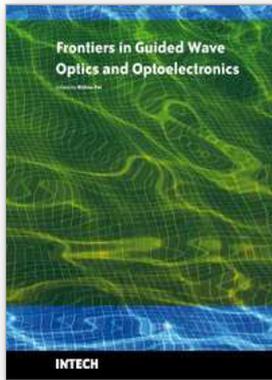
Frontiers in Guided Wave Optics and Optoelectronics
Edited by Bishnu Pal

ISBN 978-953-7619-82-4
Hard cover, 674 pages
Publisher InTech
Published online 01, February, 2010
Published in print edition February, 2010

As the editor, I feel extremely happy to present to the readers such a rich collection of chapters authored/co-authored by a large number of experts from around the world covering the broad field of guided wave optics and optoelectronics. Most of the chapters are state-of-the-art on respective topics or areas that are emerging. Several authors narrated technological challenges in a lucid manner, which was possible because of individual expertise of the authors in their own subject specialties. I have no doubt that this book will be useful to graduate students, teachers, researchers, and practicing engineers and technologists and that they would love to have it on their book shelves for ready reference at any time.

How to reference
In order to correctly reference this scholarly work, feel free to copy and paste the following:

Bishnu P. Pal (2010). Application Specific Optical Fibers, Frontiers in Guided Wave Optics and Optoelectronics, Bishnu Pal (Ed.), ISBN: 978-953-7619-82-4, InTech, Available from: http://www.intechopen.com/books/frontiers-in-guided-wave-optics-and-optoelectronics/application-specific-optical-fibers

INTECH
open science | open minds